



X International Voevodsky Conference "Physics and  
Chemistry of Elementary Chemical Processes" (VVV-2022)

2022 Novosibirsk 05-09 Sep 2022



**Effect of dihalide substituents on crystal structure and magnetic  
properties of cation  $[\text{Mn}^{\text{III}}(3,5\text{-diHal-sal}_2\text{323})]^+$  complexes  
with  $\text{BPh}_4$  anion**

*Kazakova Anna Vladimirovna*

*Federal Research Center of Problems of Chemical Physics and Medicinal Chemistry RAS,  
Academician Semenov avenue 1, 142432, Chernogolovka, Russia*

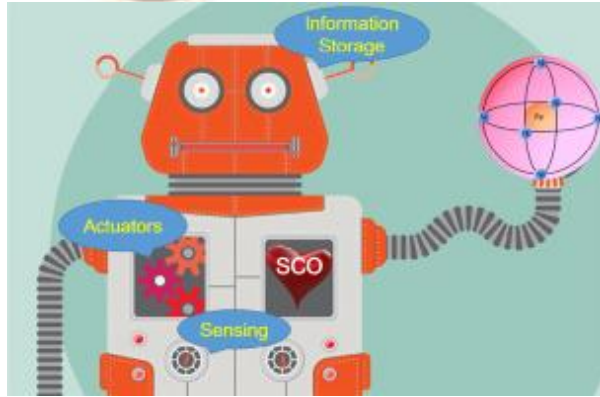
*E-mail: [kazakova@icp.ac.ru](mailto:kazakova@icp.ac.ru)*



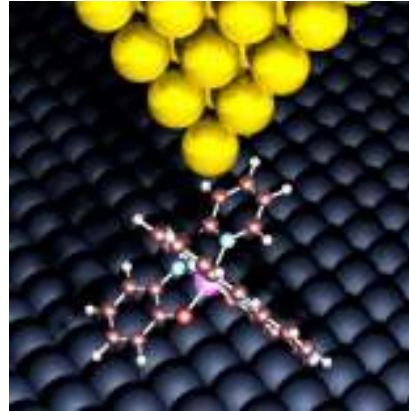
# Application of spin-crossover compounds in modern electronic devices



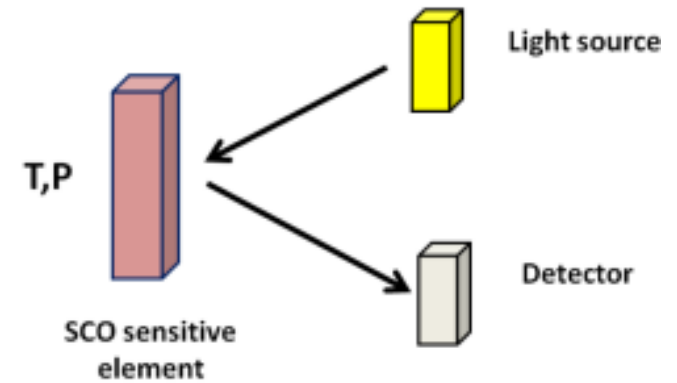
➤ One molecule is one information bit



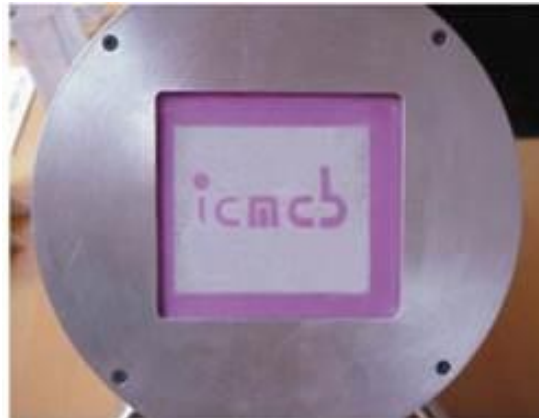
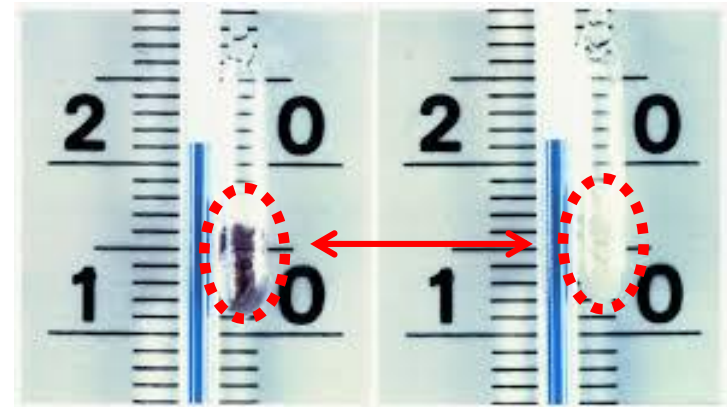
➤ Display



➤ Sensors



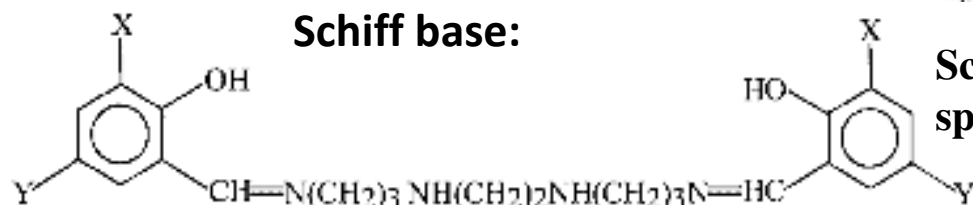
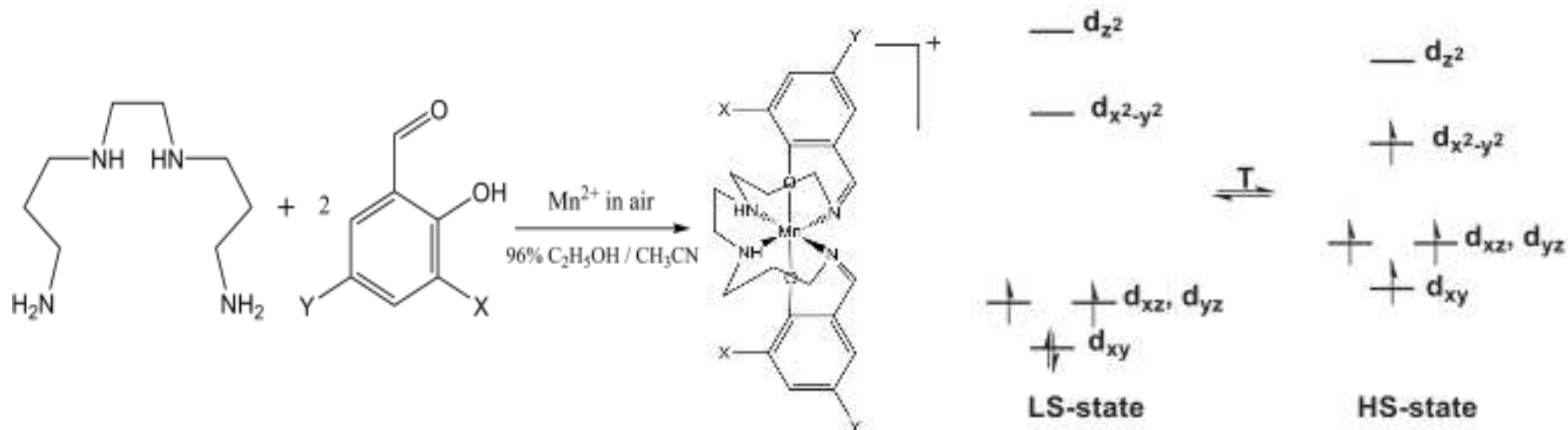
➤ Thermochromism



# Spin-crossover complex based on Mn(III)

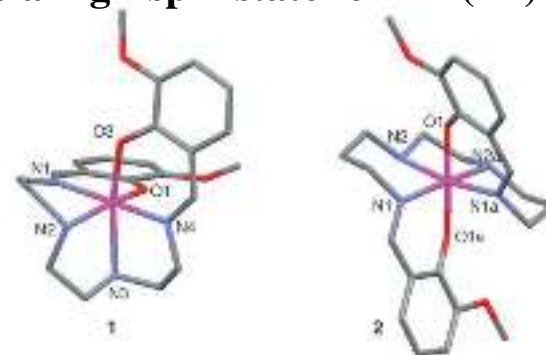
The first Mn(III) spin-crossover complex was synthesized in 2003.

Scheme of synthesis of Mn(III) spin-crossover complex:



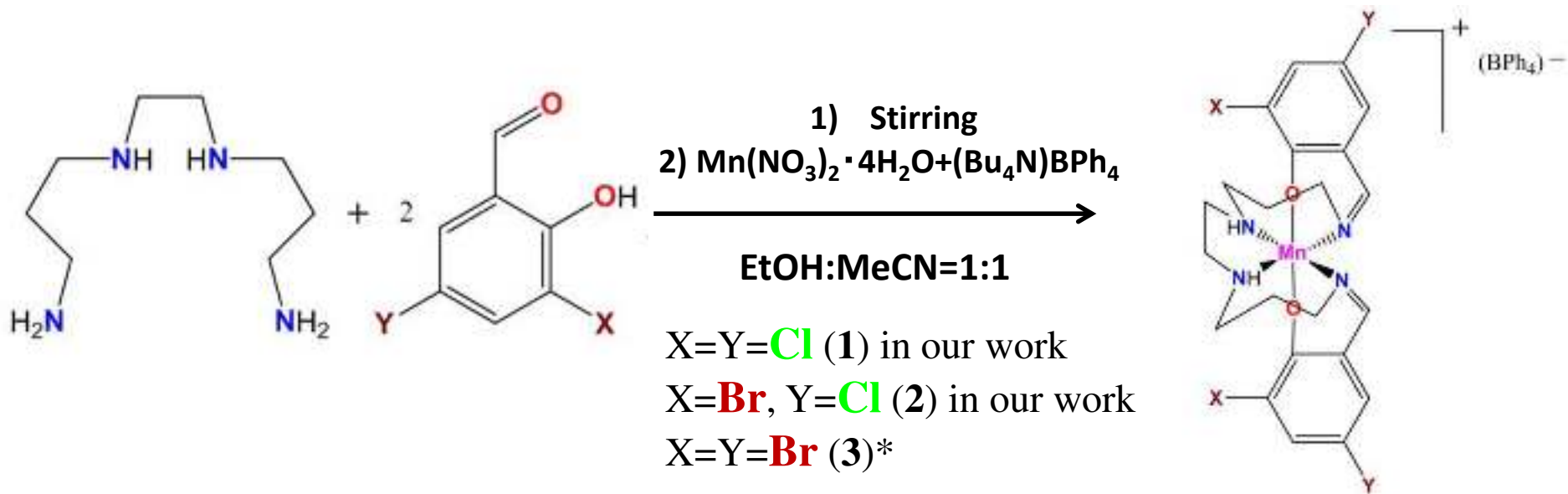
Scheme of the electron transition from a low-spin state to a high-spin state for Mn(III)

	X	Y	Ligand
1	H	H	H <sub>2</sub> (sal-N-1,5,8,12) [H <sub>2</sub> L <sup>1</sup> ]
2	H	Cl	H <sub>2</sub> (5-Cl-sal-N-1,5,8,12) [H <sub>2</sub> L <sup>2</sup> ]
3	H	Br	H <sub>2</sub> (5-Br-sal-N-1,5,8,12) [H <sub>2</sub> L <sup>3</sup> ]
4	OCH <sub>3</sub>	H	H <sub>2</sub> (3-methoxy-sal-N-1,5,8,12) [H <sub>2</sub> L <sup>4</sup> ]

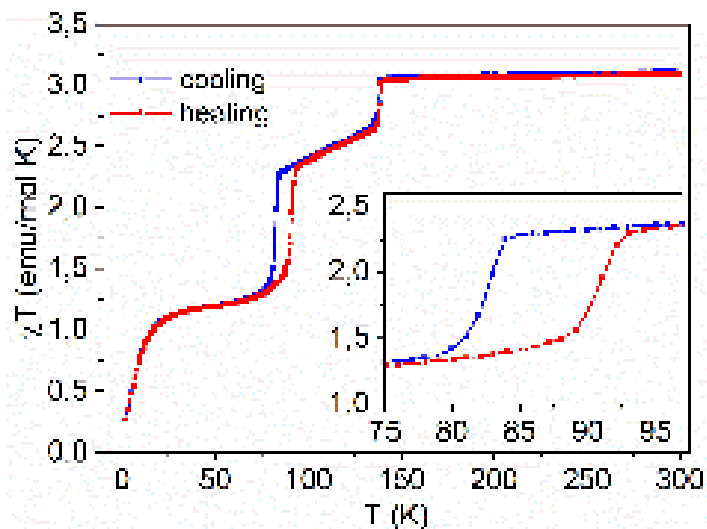
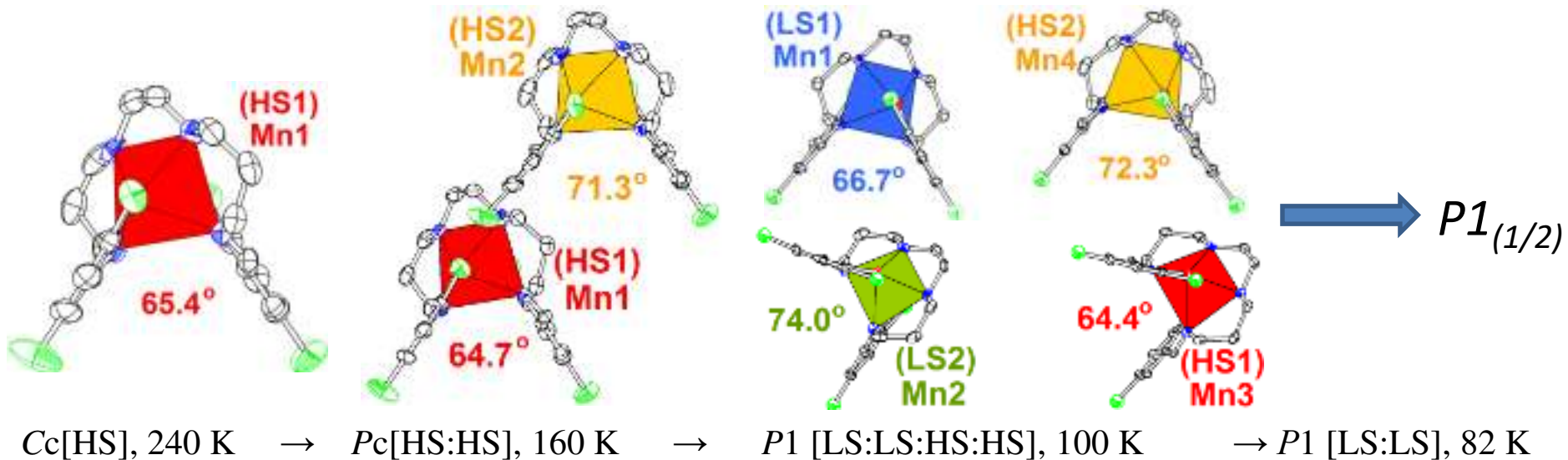


**Axial compression of Mn(III) coordination sphere during the transition to spin-crossover**

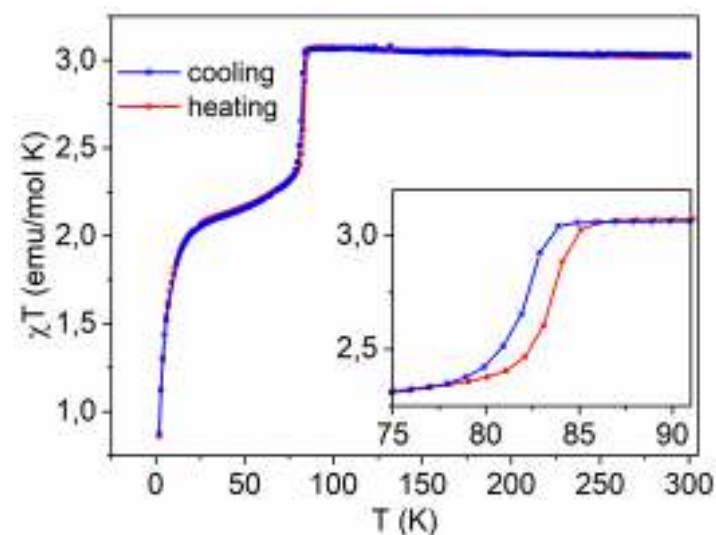
# Scheme of synthesis of complexes of the form [Mn<sup>III</sup>(diHal-sal<sub>2</sub>323)]BPh<sub>4</sub>



Compound		C(%)	H(%)	N(%)
(1)	Calc.	61,91	4,97	6,28
	Exp.	61,46	4,96	6,25
(2)	Calc.	56,30	4,52	5,70
	Exp.	57,47	4,64	5,91

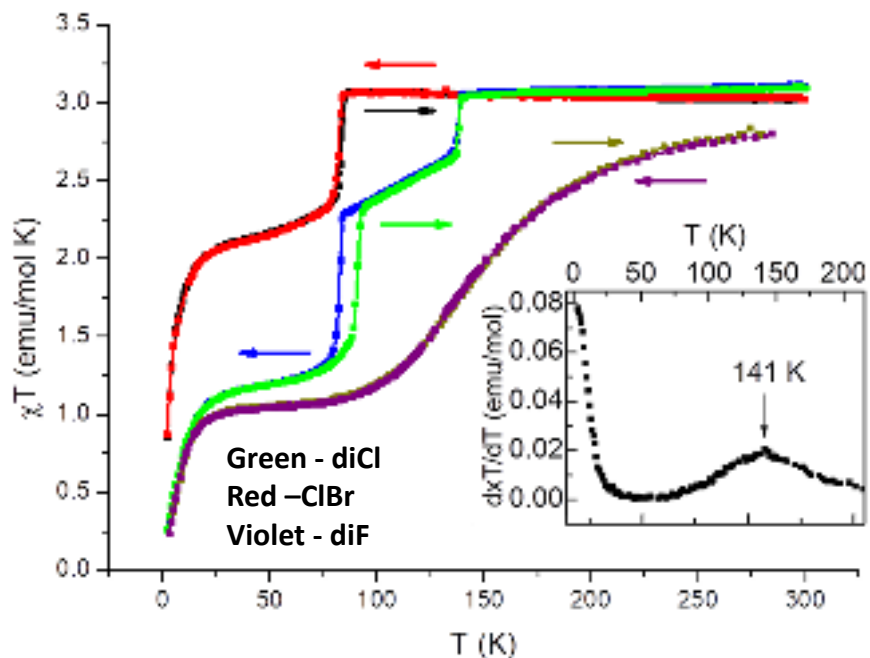


Temperature dependence of  $\chi T$  product for  $[Mn(3,5-Br,Cl-sal_2-323)]BPh_4$  in cooling (blue curve) and heating (red curve) modes with the inset showing the 8 K wide hysteresis transition.

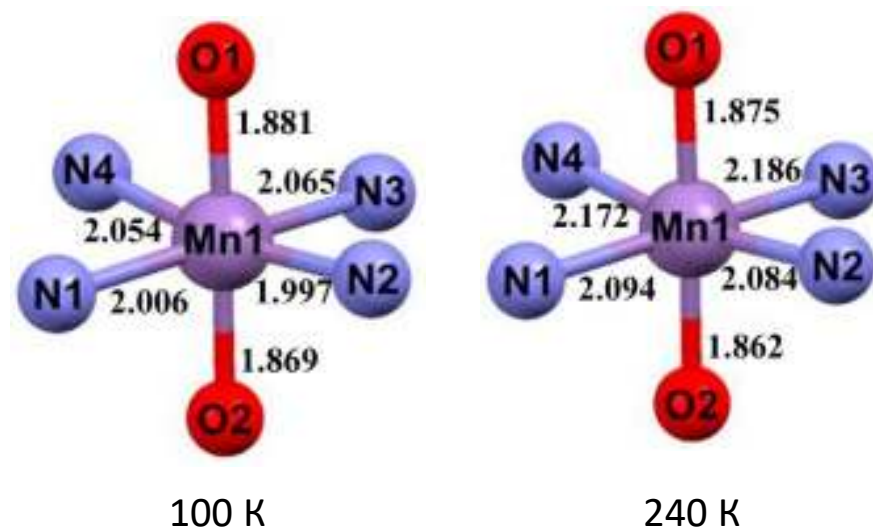


Temperature dependence of  $\chi T$  product for  $[Mn(3,5-Br,Cl-sal_2-323)]BPh_4$  in cooling (blue curve) and heating (red curve) modes with the inset showing the 2 K wide hysteresis transition.

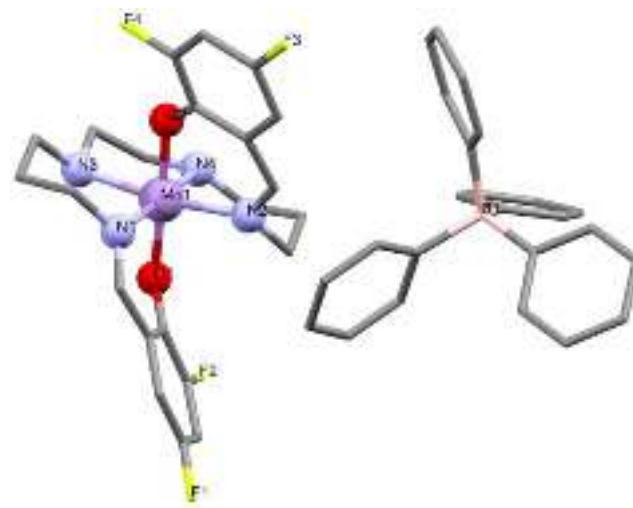
# Structure and properties of $[\text{Mn}(\text{3,5-diF-sal}_2\text{323})]\text{BPh}_4$



Temperature dependence of  $\chi T$  product for  $[\text{Mn}(\text{3,5-diHal-sal}_2\text{-323})]\text{BPh}_4$  in cooling and heating.



The coordination sphere of the Mn(III) ion in the  $[\text{Mn}(\text{3,5-diF-sal}_2\text{-323})]\text{BPh}_4$  complex at 100 and 240 K.



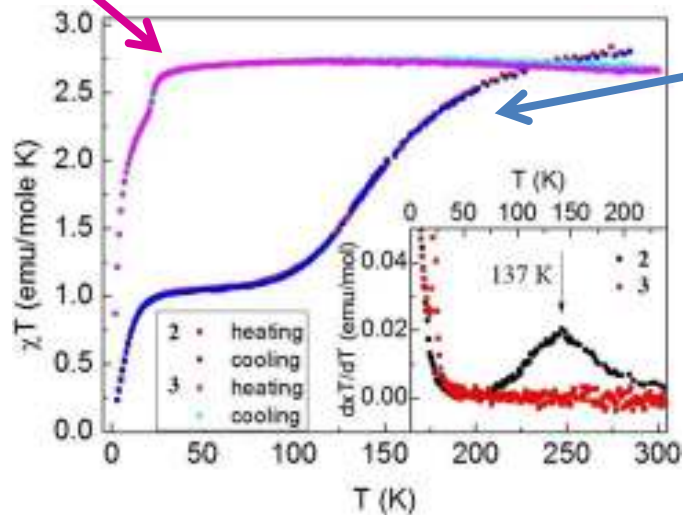
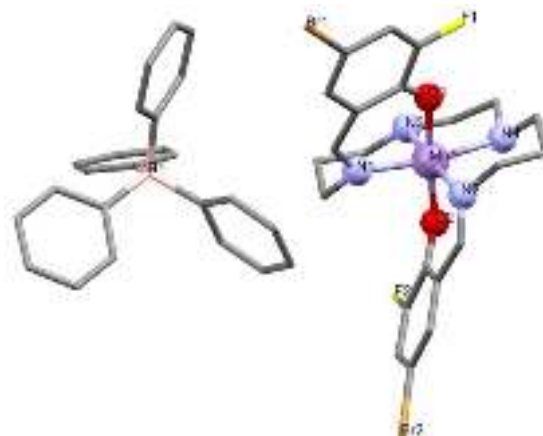
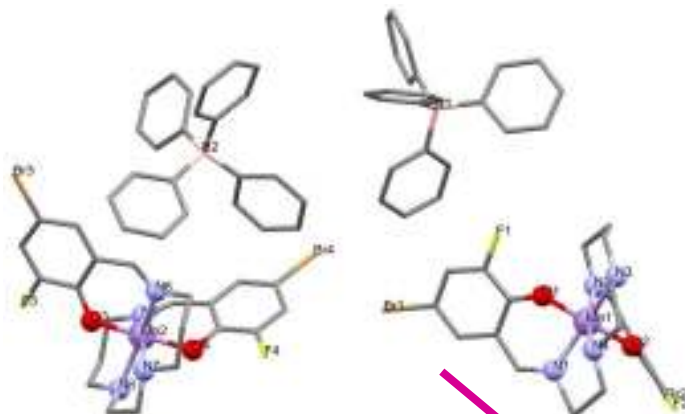
The general view of asymmetric units of compound **diF**. H atoms are omitted for clarity.

# The synthesis of the new polymorphic modifications [Mn(3,5-F-Br-sal<sub>2</sub>323)]BPh<sub>4</sub>



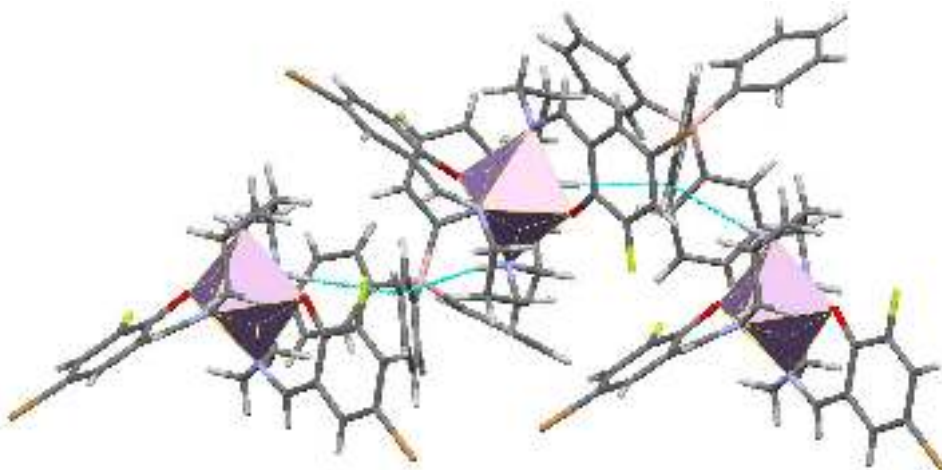
Triclinic phase

Monoclinic phase

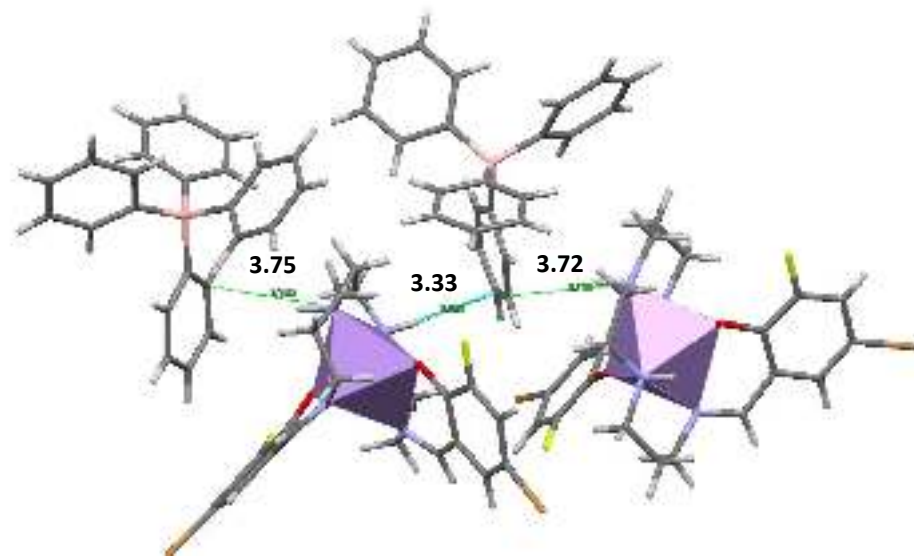


Temperature dependences of  $\chi_m T$  product for **Triclinic** and **Monoclinic** phases in cooling and heating modes. Inset:  $d(\chi_m T)/dT$  vs.  $T$ .

# Comparison of crystal structures of two polymorphic modifications [Mn(3,5-F-Br-sal<sub>2</sub>323)]BPh<sub>4</sub>



N-H $\cdots\pi_{\text{ph}}\cdots$ H-N interactions between [Mn(3,5-FBr-sal<sub>2</sub>323)]<sup>+</sup> and BPh<sub>4</sub><sup>-</sup> units, where N $\cdots$ C distances lie in the range of 3.26–3.40 Å K in **monoclinic phase**



Discrete N-H $\cdots$ C interactions (cyan lines) in **triclinic phase**. Green lines show the large distance N-H $\cdots$ C between cations and anions in **triclinic phase** (values in Å).

## Conclusion:

- New Mn(III) complexes with ligands of the sal<sub>2</sub>323 family containing two F, Cl or F and Br in positions 3 and 5 of the phenolate nucleus have been synthesized: [Mn(3,5-diF-sal<sub>2</sub>323)]BPh<sub>4</sub> (**1**), [Mn(3,5-F,Br-sal<sub>2</sub>323)]BPh<sub>4</sub> (**2**, monoclinic) and (**3**, triclinic). [Mn(3,5-diCl-sal<sub>2</sub>323)]BPh<sub>4</sub> (**4**), [Mn(3,5-Br,Cl-sal<sub>2</sub>323)]BPh<sub>4</sub> (**5**).
- Careful evaluation of the supramolecular structure of the complexes revealed strong correlation between the supramolecular packing forces and their magnetic properties.
- The nature of the dihaloid substituents and their position on the phenolate nuclear have a strong effect on the structure and magnetic properties of the Mn(III) complexes with the tetraphenylborate anion.
- The first polymorphic modifications among Mn(III) complexes with ligands of the sal<sub>2</sub>323 family have been synthesized.

# Acknowledgements:

- Prof. Yagubskii E.B.,
- Dr. Korchagin D.V.,
- Dr. Shilov G.V.
- Tiunova A.V.
- Prof. Vasiliev A.N.
- Zacharov K.V.

We acknowledge funding from the Ministry of Science and Higher Education of the Russian Federation (Grant No. 075-15-2020-779).

thank you for your attention

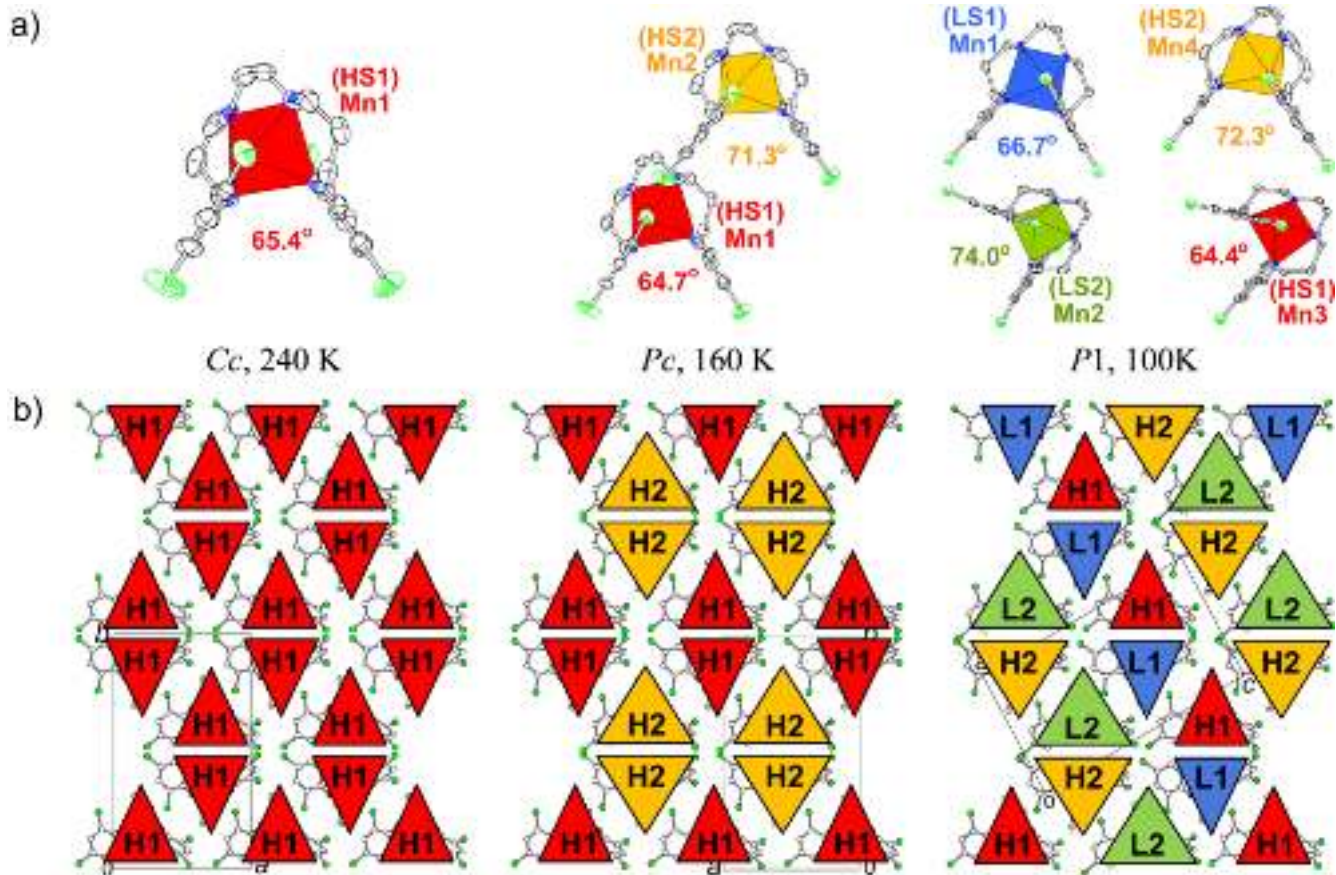


**Figure.** Crystal structures of complex diCl in *Cc* (240 K), *Pc* (160 K) and *P1* (100 K) phases ( $\text{BPh}_4$  anions and H atoms are omitted for clarity). a) Independent  $[\text{Mn}(\text{3,5-diCl-sal-n-1,5,8})]^+$  cations with distorted  $\text{MnN}_4\text{O}_2$  units shown as polyhedra. b) Schematic viewing of the SCO cations packing. Narrow and wide triangles mark smaller and larger angles between two average phenolate planes ( $\text{NOC}_7\text{Cl}_2$ ) of 3,5-diCl-sal-N-1,5,8,12 ligand in the cations. L1, L2 and H1, H2 correspond to the low spin and high spin cations, respectively.

# The synthesis of the new polymorphic modifications [Mn(3,5-F-Br-sal<sub>2</sub>323)]BPh<sub>4</sub>

Monoclinic

Triclinic

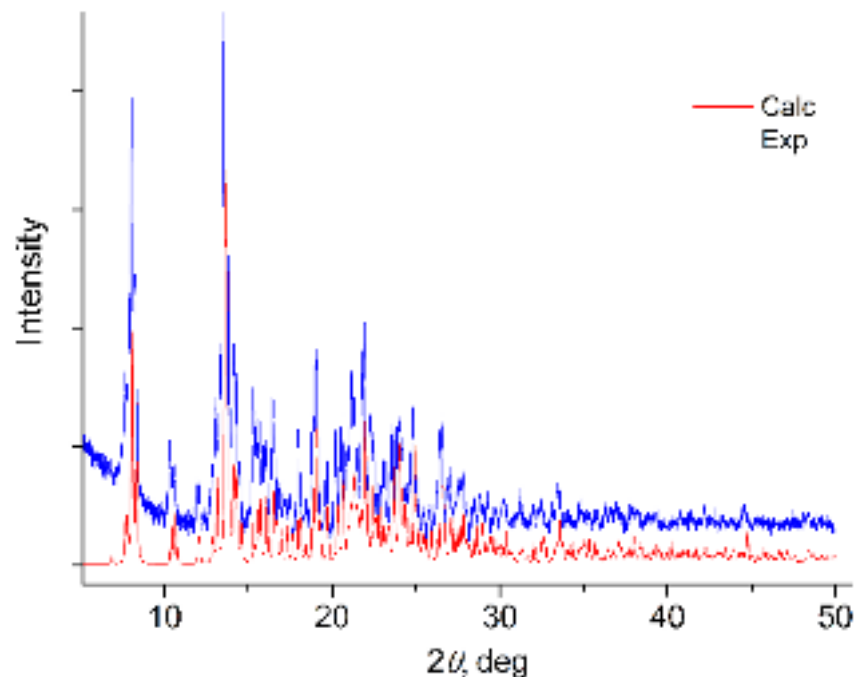
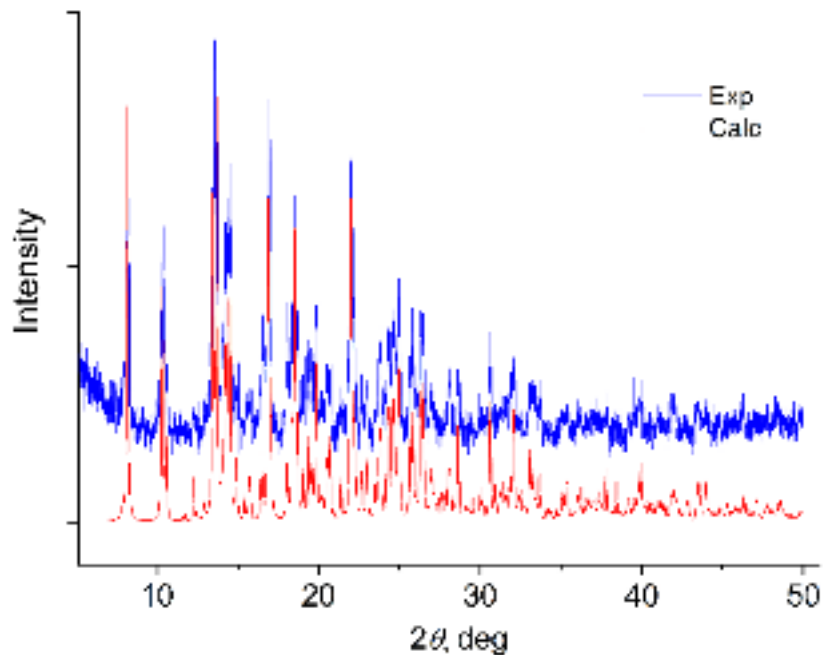


**Figure.** Powder X-ray diffraction pattern of polycrystalline samples of **5** and **6** : experimental (blue), and calculated from single crystal data (red).

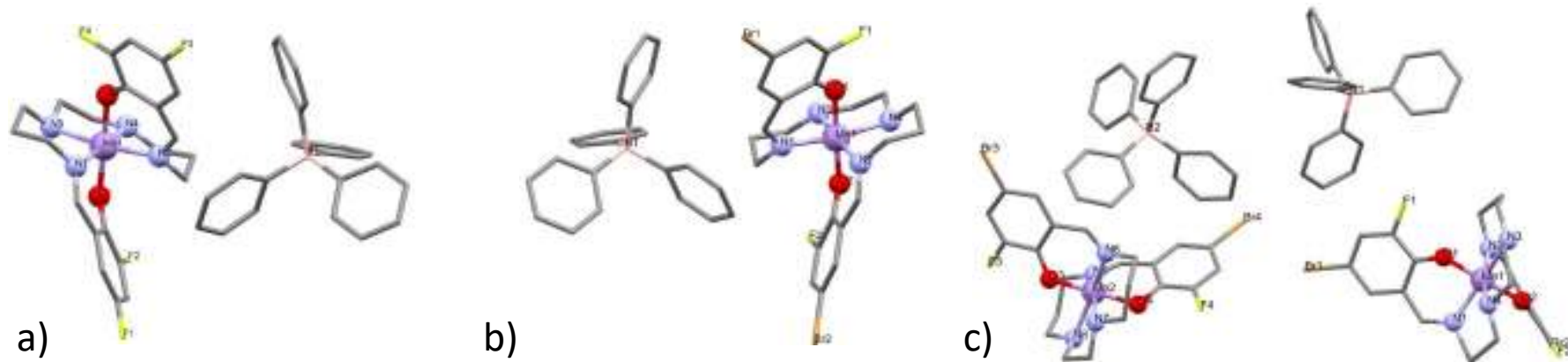


**Figure 9.** The general view of asymmetric units of compound **3(a)**, **4(b)** and **5(c)**. H atoms are omitted for clarity.

**Table 1.** Selected bond lengths and octahedral distortion parameters in **3-5**<sup>[a]</sup>

Parameter/Temp	3			4			5		
	100K	160K	240K	100K	160K	240K	100K (Mn1/Mn2)	160K(Mn1/Mn2)	240K(Mn1/Mn2)
Mn-O, Å	1.875(1)	1.870(1)	1.889(2)	1.871(2)	1.865(2)	1.883(2)	1.872(7) / 1.873(7)	1.874(7) / 1.888(7)	1.877(8) / 1.864(8)
<u>Mn-N</u> , Å	2.001(1)	2.050(2)	2.089(2)	2.001(2)	2.064(3)	2.097(3)	2.115(9) / 2.104(9)	2.120(8) / 2.102(8)	2.12(1) / 2.12(1)
Mn-N <sub>ax</sub> , Å	2.059(1)	2.128(2)	2.179(2)	2.061(2)	2.146(3)	2.192(3)	2.229(9) / 2.203(9)	2.235(9) / 2.205(9)	2.21(1) / 2.20(1)
Σ, °	34.0	48.6	58.5	35.4	55.5	84.8	69.8 / 86.8	89.5 / 88.1	70.4 / 68.3
Θ, °	106.8	160.1	198.8	106.2	175.4	210.1	260.8 / 230.7	258.9 / 235.0	259.4 / 237.4
ζ, Å	0.414	0.584	0.708	0.427	0.642	0.748	0.802 / 0.748	0.809 / 0.764	0.769 / 0.775

[a] Σ is the sum of the deviation from 90° of the 12 cis-angles of the MnN<sub>4</sub>O<sub>2</sub> octahedron Θ is the sum of the deviation from 60° of the 24 trigonal angles of the projection of the MnN<sub>4</sub>O<sub>2</sub> octahedron onto the trigonal faces. ζ is the distance distortion parameter, which is the sum of deviation from individual M-X bond distances with respect to the mean metal-ligand bond distance.